

Electron-impact ionization of the chlorine molecule

Pietro Calandra, Caroline S. S. O'Connor, and Stephen D. Price

Citation: *The Journal of Chemical Physics* **112**, 10821 (2000); doi: 10.1063/1.481753

View online: <http://dx.doi.org/10.1063/1.481753>

View Table of Contents: <http://scitation.aip.org/content/aip/journal/jcp/112/24?ver=pdfcov>

Published by the AIP Publishing

Articles you may be interested in

[Theoretical Treatment of Electron-Impact Ionization of Molecules](#)

AIP Conf. Proc. **811**, 72 (2006); 10.1063/1.2165623

[An elementary method for calculating orientation-averaged fully differential electron-impact ionization cross sections for molecules](#)

J. Chem. Phys. **123**, 204302 (2005); 10.1063/1.2118607

[Comment on the accuracy of absolute electron-impact ionization cross sections for molecules](#)

J. Chem. Phys. **114**, 4741 (2001); 10.1063/1.1346641

[Electron-impact ionization cross sections for polyatomic molecules, radicals, and ions](#)

AIP Conf. Proc. **543**, 220 (2000); 10.1063/1.1336281

[Electron-impact ionization cross sections of atmospheric molecules](#)

J. Chem. Phys. **106**, 1026 (1997); 10.1063/1.473186

A promotional banner for AIP Applied Physics Reviews. On the left is a thumbnail image of a journal cover titled 'AIP Applied Physics Reviews' featuring a diagram of a device. The background is a blue gradient with a molecular model of spheres and sticks. The text 'NEW Special Topic Sections' is prominently displayed in white. Below this, 'NOW ONLINE' is written in orange, followed by 'Lithium Niobate Properties and Applications: Reviews of Emerging Trends' in white. The AIP Applied Physics Reviews logo is in the bottom right corner.

NEW Special Topic Sections

NOW ONLINE
Lithium Niobate Properties and Applications:
Reviews of Emerging Trends

AIP Applied Physics Reviews

Electron-impact ionization of the chlorine molecule

Pietro Calandra,^{a)} Caroline S. S. O'Connor, and Stephen D. Price^{b)}

Department of Chemistry, University College London, 20 Gordon Street, London WC1H 0AJ, United Kingdom

(Received 12 January 2000; accepted 30 March 2000)

Relative partial ionization cross sections for the formation of Cl_2^+ , Cl^+ and Cl^{2+} from molecular chlorine have been recorded as a function of the ionizing electron energy. In these measurements particular attention has been paid to the efficient collection of fragment ions with high translational energies and the minimization of any mass-dependent discrimination effects. The cross sections show that at electron energies above the double ionization threshold the yield of fragment ions can be comparable with the ion yield of nondissociative ionization. Further analysis shows that at electron energies above 50 eV the yield of fragment ions from multiple ionization is comparable with the yield of fragment ions from single ionization: dissociative multiple ionization contributes 14% of the ion yield at 50 eV electron energy and 26% at 100 eV. The decay of Cl_2^{2+} by heterolytic cleavage to form Cl^{2+} is a result of approximately 5% of the dissociative double ionization events. This heterolytic process has a threshold of 41.8 ± 1.5 eV. Electron-impact induced triple ionization to form long-lived Cl_2^{3+} ions has been detected for the first time. This nondissociative triple ionization process makes up approximately 2% of the triple ionization events and triple ionization is responsible for approximately 2% of the ion yield above 100 eV. The threshold for dissociative triple ionization is determined to be 65.3 ± 1.5 eV, a value in good agreement with a trication precursor state energy derived from the kinetic energy release for the fragmentation of Cl_2^{3+} to Cl^{2+} and Cl^+ , which provides the first experimental estimate of the triple ionization energy of molecular chlorine. © 2000 American Institute of Physics. [S0021-9606(00)01224-1]

I. INTRODUCTION

Molecular chlorine is used in plasma etching.¹ In this process the chlorine atoms produced in a gas discharge efficiently etch a silicon substrate. One of the dominant pathways following the electron/ Cl_2 interactions in the plasma is ionization, both dissociative and nondissociative.²⁻⁵ However, the lack of quantitative data on the dissociative ionization of chlorine by electron-impact has been noted in the recently assembled library of data quantifying the consequences of the interaction of electrons with Cl_2 .⁶ Such data is essential for modeling chlorine plasmas in order to gain a more detailed understanding of the etching process.⁶ The investigation of the electron-impact ionization of the chlorine molecule described in this paper, quantifying the ions produced following the ionization process as a function of electron energy, provides the first step in filling this significant gap in our understanding of electron interactions with Cl_2 .

The measurement of accurate partial ionization cross sections presents some fundamental difficulties in addition to those involved in determining a total ionization cross section.^{7,8} By definition, one must identify the products formed following ionization events, not just count positively charged species. Thus, to measure a partial ionization cross section a mass spectrometric experiment is required. Using a mass spectrometer to count ions to produce a partial ioniza-

tion cross section one must ensure that the apparatus is detecting all the ions, regardless of their mass or initial kinetic energy, with equal efficiency. It is becoming apparent that early investigations of partial ionization cross sections, involving quadrupoles or commercial magnetic sector instruments, did not detect the energetic fragment ions formed by dissociative multiple ionization [e.g., Eqs. (1) and (2)] very efficiently⁸⁻¹²



In these early experiments, even if the problem of the efficient detection of energetic ions was recognized, the loss of a significant proportion of such signals was considered to be of little importance, as it was commonly thought that multiple ionization provides only a small contribution to the total ion yield.⁷ However, in recent years, experiments that allow the efficient collection of high energy ions have shown that energetic ions from multiple ionization can contribute significantly to the ion yields following photon or electron impact ionization of small molecules.^{8,10-15} For example, recently revised data for the ionization of CF_4 shows that multiple ionization contributes 17% of the ion yield at 100 eV and 43% at 200 eV.^{12,13} Hence, it is possible that early studies of branching ratios, or partial ionization cross sections, underestimated the degree of dissociative ionization by missing the contribution of dissociative multiple ionization to the total ion yield.

^{a)}Current Address: University of Palermo, Viale Delle Scienze, Parco D'Orleans 2, 90100, Italy.

^{b)}Electronic mail: s.d.price@ucl.ac.uk

In this work we use two-dimensional time-of-flight (TOF) mass spectrometry^{13,16,17} to study the ionization of Cl_2 . This technique allows us to detect and identify the ions formed following the interaction of electrons with Cl_2 and to assess our detection efficiency for these ions. The technique also allows us to distinguish and quantify the contribution to the total ion yield from multiple ionization, under conditions where we can precisely assess our detection efficiency. In this study, the energy independent collection efficiency of the time-of-flight technique is augmented by a rigorous attempt to minimize any mass or charge-state dependent discrimination in the experiment. Such effects have been shown by previous investigations to considerably affect the relative abundances of fragment ions in TOF mass spectra.¹⁸

As identified by Christophorou and Olthoff in their survey of data quantifying the consequences of electron interactions with Cl_2 , mass spectrally resolved studies of the electron impact ionization of this molecule are rare.⁶ The threshold for Cl^+ formation from Cl_2 was first determined as 15.51 ± 0.03 eV close to 40 years ago^{19,20} and one of these early studies also measured various thresholds for the population of the ground and nondissociative excited states of Cl_2^+ .¹⁹

Multiply charged states of small stable molecules are normally, but not exclusively, thermodynamically unstable with respect to charge-separated products.²¹ However, despite this thermodynamic instability, long-lived (metastable) multiply charged states of small molecules are well known.^{22–25} In these states the bonding interaction is sufficient to overcome the Coulombic repulsion between the positive charges, and there has been a recent upsurge of interest in studying the properties and reactivity of such long-lived multiply charged ions.^{23,26–29} For Cl_2 , Heron and Diebler³⁰ observed long-lived Cl_2^{2+} ions in electron-impact mass spectra in 1960 and determined their appearance energy as 32.6 eV. This observation was rationalized when *ab initio* calculations showed that the ground state of Cl_2^{2+} possessed a significant metastable well.³¹ Eleven years later, the charge-separating predissociation [Eq. (2)] of long-lived Cl_2^{2+} ions was observed in the field free region of a twin-sector mass spectrometer and the kinetic energy release for this process was evaluated.³² A more detailed investigation of the electronic structure of Cl_2^{2+} was performed by Fournier *et al.*³³ using double-charge transfer (DCT) spectroscopy, coupled with extensive configuration interaction calculations. The relative energies of the states of Cl_2^{2+} calculated by Fournier *et al.*³³ agree well with the energies of the 6 singlet states below 40 eV they derived from their DCT spectra. More recently, threshold photoelectrons coincidence (TPEsCO) spectroscopy, coupled with synchrotron radiation, has been used to record a threshold photoelectron spectrum³⁴ of the formation of Cl_2^{2+} . This experiment gives the vertical ionization energy (31.13 eV) for populating the ground state of the dictation and resolved 5 distinct vibrational levels in the metastable potential well of this electronic state. The TPEsCO spectrum also showed the population of the first 3 excited states of Cl_2^{2+} by double photoionization, although no vibrational structure was observed in these signals.³⁴

In this work we have recorded two-dimensional TOF

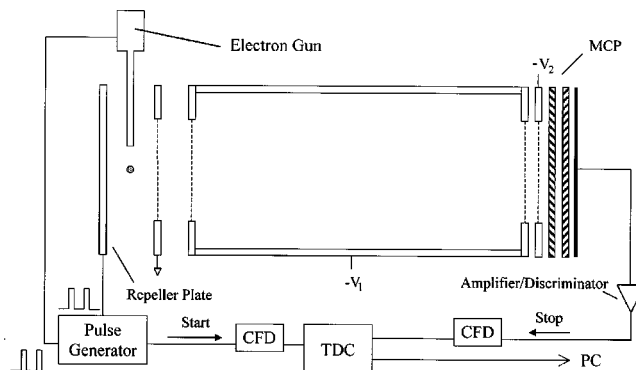


FIG. 1. Schematic of the time-of-flight mass spectrometer used to record the one-dimensional and two-dimensional mass spectra. As described in the text, and indicated in the figure, both the electron-gun and the repeller plate are pulsed. Ion signals from the microchannel plate (MCP) detector pass through a constant fraction discriminator (CFD) to a time-to-digital converter (TDC).

mass spectra following electron impact ionization of molecular chlorine from at electron energies 25–200 eV. Using a data analysis procedure which distinguishes both the contribution of both multiple and single ionization to the yield of a given species, we can quantify the contribution of single, double and triple ionization to the relative yields of the Cl_2^+ , Cl^+ , and Cl_2^{2+} ions which dominate the mass spectrum of Cl_2 . For example, we show that the formation of Cl_2^{2+} from Cl_2^{2+} contributes significantly to the ion yield. In addition, we observe for the first time the population of long-lived states of Cl_2^{3+} following electron-impact ionization.

II. EXPERIMENT

A. Experimental apparatus

All the experiments described in this paper were performed on a Wiley–McClaren³⁵ style time-of-flight mass spectrometer (TOFMS) which is shown schematically in Fig. 1. Recently, considerable improvements have been made to both the experimental apparatus and the data collection electronics. Specifically, the installation of a 40 mm diameter microchannel plate detector, the construction of a new electron gun which can produce short pulses of ionizing electrons at a high repetition rate and the commissioning of a fast data collection system. The aim of these improvements was twofold: to increase and better quantify our detection efficiency for fragment ions formed with high kinetic energies and to allow the recording of two-dimensional ion–ion coincidence spectra following the formation and dissociation of multiply charged ions by the pulse of ionizing electrons. Such spectra have been shown to be powerful probes of both the dynamics and energetics of the fragmentation processes of a variety of multiply-charged and singly-charged ions.^{13,36–43} The operation of the upgraded apparatus and the spectra that can now be recorded are described in detail below.

The experiment is controlled by a pulse generator running at 50 kHz which controls the pulsing of the electron gun and the repeller plate of the TOFMS and starts the data collection electronics. At the beginning of each cycle the pulse

generator first triggers the emission of a pulse of electrons from the electron gun. The electron gun consists of a filament together with appropriate optics to extract and transport the electrons from the filament to the entrance of the needle which guides them to the ionization region of the TOFMS. Normally, the electron optics are held at potentials which stop the electrons reaching the entrance of the needle. However, on receiving the trigger from the pulse generator fast MOSFET circuitry is used to apply briefly voltages which allow electrons to reach the needle and access the ionization volume. The actual length of electron pulse resulting from this procedure is longer than the 4 ns trigger pulse due to the inductive and capacitive effects of the lens elements. However, the width of peaks in the mass spectra shows that the electron pulse is certainly shorter than 30 ns. Approximately 80 ns after the electron pulse is initiated the repeller plate of the TOFMS is pulsed to 400 V to extract the ions from the ion source and into the second electric field which accelerates the ions into the drift tube and then onto the microchannel plate detector.

Ion signals from the detector are amplified, discriminated and passed to a Le Croy 3377 time to digital converter (TDC) which has previously been triggered by the pulse generator. The TDC is capable of recording multiple stop signals each time it is triggered and is set to ignore events where it receives no ion signals following the start signal from the pulse generator. Hence, events involving multiple ion arrivals at the detector can be identified and recorded. The ion arrival times associated with successive events are accumulated in a memory module (Le Croy 4302) which is fed from the TDC via a fast FERA interface. The memory unit accumulates 16 Kbytes worth of data which is then rapidly read by a 400 MHz PC via a SCSI interface incorporated in a DDC3000/PCI crate. The use of fast FERA interfacing, coupled with data transfer using a SCSI bus, allows this system to gather data at over 50 kHz, a factor of 200 times faster than our earlier data collection electronics which involved passing each individual event to the PC via a GPIB interface.

B. Mass discrimination effects

In extracting quantitative data from the mass spectra which are produced by our experimental apparatus one must carefully confirm that no mass discrimination effects exist. The importance of a variety of subtle effects which can generate mass discrimination in time of flight spectra has been discussed by Bruce and Bonham.¹⁸ Specifically, they found the relative intensity of Ar^{2+} and Ar^+ following electron-impact ionization of argon depended on the background argon pressure, the energy with which the ions hit the MCP detector and the setting of the constant fraction discriminator used in their data collection system. We have investigated the performance of our new apparatus by measuring the relative intensities of the Ar^{2+} to Ar^+ ions detected following ionization of argon, along identical lines to that of Bruce and Bonham, to ensure we operate under conditions where none of the effects they identified are influencing our ion yields. As with the study of Bruce and Bonham, we find the experimental value of the Ar^{2+} to Ar^+ yield depends on the parameters listed above.¹⁸ However, we can find a region of ex-

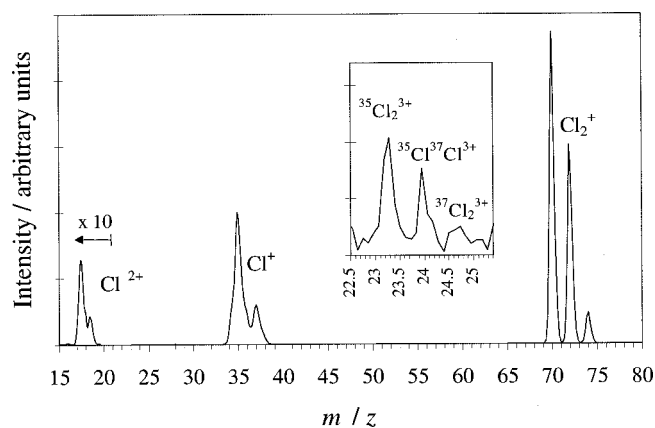


FIG. 2. Representative mass spectrum of molecular chlorine recorded at an ionizing electron energy of 200 eV. As indicated in the figure, the intensity-scale has been expanded by a factor of 10 below an m/z value of 20. The inset is an expanded ($\times 400$) portion of the mass spectrum to show the signals due to Cl_2^{3+} .

perimental parameter space where the Ar^{2+} to Ar^+ ratio is independent of these variables. Under these conditions we determine an Ar^{2+} to Ar^+ ratio which agrees, within the respective error limits, with the value determined by Bruce and Bonham,¹⁸ and these are the conditions under which we recorded the data which is presented below.

Any energy dependent discrimination effects in our experiment are easy to assess using the geometry of the TOFMS and the flight time of the ions from the ionization volume to the detector. Given that ionization occurs in the center of the source region, then all ions with a translational energy of less than 12 eV will hit the detector. Ions with a higher translational energy will not be detected if they have an energy component perpendicular to the axis of the mass spectrometer of greater than 12 eV. However, the “flat-topped” shape of the coincidence signals we detect in the two-dimensional spectrum shows that ions with kinetic energies above 12 eV are not formed in significant numbers by the double and triple ionization processes which dominate the multiple ionization cross section at the energies of the reported investigations.

C. Data processing

The data produced from multiple coincidence spectroscopy, and its interpretation, has been described in considerable detail in the literature.^{13,36–43} Briefly, the data accumulated by the TDC is a list of ion arrival times associated with each pulse of the repeller plate. Due to the higher relative probability of single ionization with respect to multiple ionization, the majority of such “events” involve the arrival of just one ion. We term these events singles and their arrival times are histogrammed to produce the singles mass spectrum (Fig. 2). The mass scale of this singles spectrum can easily be calibrated by recording the mass spectrum of a reference species under the same voltage conditions, and the relative ion intensities $I[X^+]$ determined by summing the counts in each peak.

Events involving multiple ion arrivals are stored individually for off-line inspection and processing. In principle,

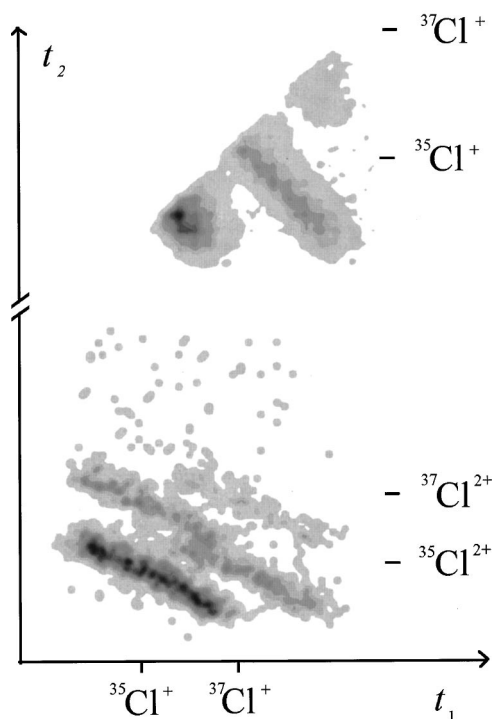


FIG. 3. Signals in the pairs spectrum following multiple ionization of Cl_2 with 200 eV electrons. As described in the text, a portion of the $\text{Cl}^+ + \text{Cl}^+$ signal is lost near $t_1 = t_2$ due to the dead time (32 ns) of the electronics.

the data collection electronics can record events with 4 or more ion arrivals. Reassuringly, in this study of the ionization of Cl_2 , where at most just two individual ions can be formed from each ionization event, the number of events involving more than 2 ion arrivals was negligible. Two-dimensional mass spectra (sometimes called pairs spectra or correlations spectra) identifying the dissociation processes occurring (Fig. 3) are easily generated from the multiple-arrivals data by constructing a two-dimensional histogram of the flight times of both ions in the ion pair. A typical spectrum is shown in Fig. 3 where the fragmentation process of Cl_2^{2+} and Cl_2^{3+} are clearly visible. As discussed below, the relative intensity of these different fragmentation channels can be assessed by summing the counts in the individual peaks. Note that, due to the deadtime of the discrimination circuitry, no pairs will be recorded if the second ion arrives within 32 ns of the first ion. This results in a “dead region” in the pairs spectrum (Fig. 3). When quantifying the yields of the reactions contributing to the pairs spectrum, the counts that are lost in this “dead region” are estimated by extrapolating the flat-topped peaks back to $t_1 = t_2$.^{13,44}

As has been discussed extensively in the literature, such two-dimensional spectra also contain a contribution from “accidental coincidences” where two ions which did not originate from the same dissociation event are detected.^{13,44,45} The contribution of accidental coincidences to the two-dimensional mass spectra, although minimized experimentally by operating at low count rates, can easily be assessed, and then subtracted, by normalizing the two-dimensional auto-correlation function of the singles spec-

trum to a known false peak (e.g., $\text{Cl}_2^+ + \text{Cl}^+$) in the pairs spectrum.^{44,45}

One of the major advantages of two-dimensional coincidence techniques is the insight they provide into the dynamics of charge-separation reactions.^{13,36–43} However, in this study of the ionization and dissociation of a diatomic molecule where the dissociation mechanism can only be a simple bond cleavage, we focus instead on the information on the ion energetics and the relative ionization cross sections that can be derived from the spectra we record.

D. Data reduction

1. Quantifying the detected ionization processes

In our earlier mass spectrometric experiments the experimental arrangement we employed (with a small area ion detector) discriminated against the detection of energetic fragment ions, such as those produced by dissociative double ionization.⁴⁶ However, the modified experimental set-up dramatically reduces the discrimination against energetic fragment ions. Specifically, all ions with a translational energy of less than 12 eV perpendicular to the axis of the TOFMS will now hit the detector as these ions have no time to escape the ionization volume, following their creation by the electron pulse, before the repeller plate is pulsed. Therefore, highly energetic fragment ions from both single and double ionization are detected in addition to low kinetic energy ions.

For ionization of Cl_2 , the intensity of the Cl^+ signal in the singles spectrum is given by

$$I[\text{Cl}^+] = f_i N_1[\text{Cl}^+] + 2 f_i (1 - f_i) N_2[\text{Cl}^+] + f_i (1 - f_i) N_3[\text{Cl}^+] + \dots, \quad (3)$$

where f_i is the ion detection efficiency and $N_n[\text{X}^+]$ is the number of ionizing events forming the final products given in parentheses from an ionization event involving the loss of n electrons from Cl_2 . The second and third terms in (3) arise because a singly charged ion formed by dissociative multiple ionization may be detected but its correlated partner may be missed, due to our experimental ion detection efficiency being less than unity. The experimental ion detection efficiency depends on the transmission of the grids defining the electric fields in the apparatus and the less than perfect efficiency of the detector and electronics. Such events, where one of the ions of a pair is not detected, give a contribution to the singles spectrum. Similarly, neglecting quadruple and higher ionization (i.e., $n \leq 3$), we can write

$$I[\text{Cl}^{2+}] = f_i N_2[\text{Cl}^{2+}] + f_i (1 - f_i) N_3[\text{Cl}^{2+}], \quad (4)$$

$$I[\text{Cl}_2^+] = f_i N_1[\text{Cl}_2^+]. \quad (5)$$

We would like to extract from our data relative partial ionization cross sections for forming the various ions we detect; for example, the relative partial ionization for forming the fragment ion Cl^+ with respect to the parent ion Cl_2^+ at a given electron energy: $\sigma_r[\text{Cl}^+/\text{Cl}_2^+]$. By definition,

$$\sigma_r[\text{Cl}^+/\text{Cl}_2^+] = \frac{\sigma[\text{Cl}^+]}{\sigma[\text{Cl}_2^+]} = \frac{\sigma_1[\text{Cl}^+] + \sigma_2[\text{Cl}^+] + \sigma_3[\text{Cl}^+]}{\sigma_1[\text{Cl}_2^+]}, \quad (6)$$

where $\sigma[\text{X}^+]$ is the cross section for forming X^+ which can be considered as a sum of the cross sections σ_n for forming X^+ via single ionization ($n=1$), double ionization ($n=2$) and triple ionization ($n=3$). Now, under conditions of low electron flux, $N_n[\text{X}^+]$ is proportional to σ_n :

$$\sigma_n[\text{X}^+] = kN_n[\text{X}^+], \quad (7)$$

where k is a constant for a given experiment. The value of k depends on the electron flux across the source region, the target gas pressure, the duration of the experiment and the electron path length in the ionization volume. By inspection of Eqs. (3) to (7) we can see that, due to the influence of the detection efficiency, it is not easy to extract the value of the relative partial ionization cross sections directly from the values of $I[\text{Cl}^+]$, $I[\text{Cl}^{2+}]$ and $I[\text{Cl}_2^+]$. To access the partial ionization cross sections, and further cross sections which allow us to quantify the contribution to the ion yields from different levels of ionization, we need also to use the data contained in the pairs spectrum.

Considering the pairs spectrum, and again neglecting quadruple and higher levels of ionization, let $P[\text{X}^+]$ represent the number of X^+ ions detected in the pairs spectrum recorded concurrently with the singles spectrum. Then we have

$$P[\text{Cl}^+] = 2f_i^2 N_2[\text{Cl}^+] + f_i^2 N_3[\text{Cl}^+], \quad (8)$$

$$P[\text{Cl}^{2+}] = f_i^2 N_3[\text{Cl}^{2+}], \quad (9)$$

noting that $N_3[\text{Cl}^{2+}] = N_3[\text{Cl}^+]$. This then allows us to recast Eq. (6) as

$$\frac{I[\text{Cl}^+] + P[\text{Cl}^+]}{I[\text{Cl}_2^+]} = \frac{N_1[\text{Cl}^+] + 2N_2[\text{Cl}^+] + N_3[\text{Cl}^+]}{N_1[\text{Cl}_2^+]} = \sigma_r[\text{Cl}^+/\text{Cl}_2^+], \quad (10)$$

$$\frac{I[\text{Cl}^{2+}] + P[\text{Cl}^{2+}]}{I[\text{Cl}_2^+]} = \frac{N_2[\text{Cl}^{2+}] + N_3[\text{Cl}^{2+}]}{N_1[\text{Cl}_2^+]} = \sigma_r[\text{Cl}^{2+}/\text{Cl}_2^+], \quad (11)$$

giving an algorithm for extracting relative partial ionization cross sections from our data. Note that, as our experiment involves the detection of positive ions, the formation of ions pairs by electron-induced reactions such as



cannot be distinguished from fragmentation to a positive ion plus a neutral. Hence, positive ions produced via ion pair formation will be included in our partial ionization cross sections: for example, reaction (12) will contribute to $\sigma_1[\text{Cl}^+]$. This is unavoidable unless one detects both negative ions and neutrals simultaneously. However, the cross

section for reaction (12) has been determined⁴⁷ and is at least a factor of 100 smaller than the total ionization cross section.^{6,47} Hence, the contribution from ion pair formation to our cross sections is effectively negligible.

If we can determine f_i we can extend our data analysis. Using f_i we can quantify the contributions to each of the ion yields from single, double and triple ionization relative to the partial ionization cross section for forming Cl_2^+ :

$$\frac{I[\text{Cl}^+] - ((1-f_i)/f_i)P[\text{Cl}^+]}{I[\text{Cl}_2^+]} = \frac{N_1[\text{Cl}^+]}{N_1[\text{Cl}_2^+]} = \frac{\sigma_1[\text{Cl}^+]}{\sigma[\text{Cl}_2^+]}, \quad (14)$$

$$\frac{I[\text{Cl}^{2+}] - ((1-f_i)/f_i)P[\text{Cl}^{2+}]}{I[\text{Cl}_2^+]} = \frac{N_2[\text{Cl}^{2+}]}{N_1[\text{Cl}_2^+]} = \frac{\sigma_2[\text{Cl}^{2+}]}{\sigma[\text{Cl}_2^+]}, \quad (15)$$

$$\frac{P[\text{Cl}^+] - P[\text{Cl}^{2+}]}{f_i I[\text{Cl}_2^+]} = \frac{2N_2[\text{Cl}^+]}{N_1[\text{Cl}_2^+]} = \frac{\sigma_2[\text{Cl}^+]}{\sigma[\text{Cl}_2^+]}, \quad (16)$$

$$\frac{P[\text{Cl}^{2+}]}{f_i I[\text{Cl}_2^+]} = \frac{N_3[\text{Cl}^{2+}]}{N_1[\text{Cl}_2^+]} = \frac{\sigma_3[\text{Cl}^+]}{\sigma[\text{Cl}_2^+]} = \frac{\sigma_3[\text{Cl}^{2+}]}{\sigma[\text{Cl}_2^+]}. \quad (17)$$

The ion detection efficiency can be determined experimentally by recording the singles and pairs spectrum of CF_4 , for which the cross sections for forming ion pairs σ_D^{++} and individual ions σ^+ can be extracted from published data.^{12,13,48} (It seems clear that the ion pair production cross sections listed in Ref. 13 should be in units of 10^{-22} m^2 , as then these data are consistent with previously published values of these cross sections.⁴⁸ Otherwise, all of these ion pair production cross sections are larger than the cross section for forming CF_3^+ , the most intense ion in the mass spectrum.¹²) If we record the singles and pairs spectra following the ionization of CF_4 at an electron energy where triple ionization can be neglected, then ΣI the total number of ions in the singles spectrum and ΣP the total number of ions in the pairs spectrum are given by

$$\Sigma P = 2f_i^2 k \sigma_D^{++}, \quad (18)$$

$$\Sigma I = f_i k \sigma^+ + 2f_i(1-f_i)k \sigma_D^{++}. \quad (19)$$

Then

$$\frac{\Sigma P}{\Sigma I} = \frac{2f_i \sigma_D^{++}}{\sigma^+ + 2(1-f_i)\sigma_D^{++}}, \quad (20)$$

allowing a value for f_i to be determined.

2. Dication energetics

The shape of the peaks in the pairs spectrum can be interpreted to yield the kinetic energy released upon fragmentation of the parent multiply-charged ion. We extract these kinetic energy releases (KERs) by constructing the ion-ion coincidence spectrum ($t_2 - t_1$) from the pair times for the reaction under scrutiny and then performing a Monte-Carlo simulation of the dissociation process in the mass

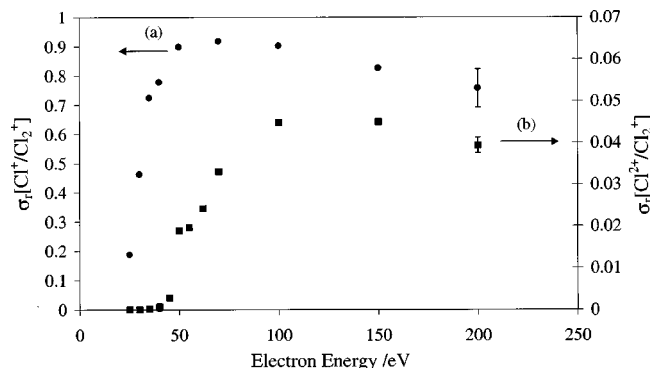


FIG. 4. Relative partial ionization cross sections for forming (a) Cl^+ and (b) Cl_2^{2+} by electron impact ionization of Cl_2 . The yield of these ions is expressed relative to the yield of Cl_2^+ . Representative error bars are shown in the figure.

spectrometer and comparing the simulated coincidence signal with the experimental data.^{46,49,50} As discussed before, using a Monte-Carlo simulation allows the inclusion of a range of apparatus parameters which affect the coincidence peak shape in the fitting procedure. The methodology and problems involved in modeling such signals have been discussed at length in the literature^{13,36,37,51} and our procedure produces KERs in excellent agreement with those in the literature.

The KERs can be used to estimate the energy of the electronic state of the multiply-charged ion $E(\text{Cl}_2^{n+})$ which dissociated to yield the fragments of interest if the asymptotic energy E_{Frag} of the dissociation limit is known:

$$E(\text{Cl}_2^{n+}) = \text{KER} + E_{\text{Frag}}. \quad (21)$$

These values of $E(\text{Cl}_2^{n+})$ can be compared with the thresholds observed in the variation of the yields of the various dissociation reactions to provide further information on the energetics of the dissociative states of Cl_2^{n+} .⁵⁰ In general, the degree of internal excitation of the fragments is not known and, hence, these estimates of the electronic state energies of Cl_2^{n+} from KER measurements should be considered as lower limits. In recent years more sophisticated methods, such as Doppler-free KER spectroscopy^{52,53} and TPEsCO,^{34,54} have been developed for the spectroscopy of individual vibronic states of dications. However, these more sophisticated techniques have been applied to only a few molecules and, hence, kinetic energy release measurements provide a readily applicable method for an initial determination of the energetics of Cl_2^{n+} .

III. RESULTS

A. Ionization yields

Experimental data were recorded at a range of ionizing electron energies between 25 and 200 eV. Figure 4 shows plots, as a function of the ionizing electron energy, of the relative partial ionization cross sections σ_r for Cl^+ and Cl_2^{2+} expressed relative to the yield of Cl_2^+ . These values were derived using Eqs. (10) and (11). The figure shows that, following the ionization of Cl_2 , the most abundant ion formed is Cl_2^+ , although between 50 and 150 eV almost as many Cl^+

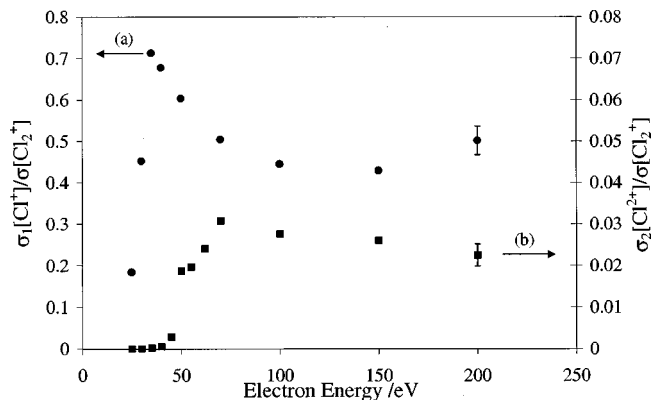


FIG. 5. Cross sections for forming (a) Cl^+ via single ionization and (b) Cl_2^{2+} via dissociative double ionization following electron-impact ionization of Cl_2 . These cross sections are expressed relative to the cross section for forming Cl_2^+ . Representative error bars are shown in the figure.

ions are formed as Cl_2^+ ions. This Cl^+ to Cl_2^+ ratio is slightly, but not dramatically, different to that (2:3) observed at comparable photon energies.⁵⁵

The threshold for Cl^+ formation is, as expected from literature data, below 25 eV and hence not reached in our experiments.^{19,20} The threshold for Cl_2^{2+} formation appears (Fig. 4) to lie between 40 eV, where within our error limits the Cl_2^{2+} yield is zero, and 45 eV where the yield is certainly nonzero. These data points thus give a determination for the threshold as 42.5 ± 2.5 eV. However, this procedure perhaps overestimates the error and using a linear extrapolation of the 3 data points lying successively above 40 eV, we estimate the threshold to be 41.8 ± 1.5 eV.

To use Eqs. (14)–(17) to derive the contribution of the different levels of ionization to the ion yields we require a value for f_i . As described above, we derive this value by recording the singles and pairs spectra following ionization of CF_4 . This procedure was repeated several times, at different electron energies, and results in a value for f_i of 0.20 ± 0.03 , in good agreement with similar quantities reported in the literature.¹⁶

Figure 5 shows the relative cross section for forming Cl^+ via single ionization [Eq. (14)] of Cl_2 . We see that the formation of Cl^+ by this route peaks at 35 eV and drops off at higher ionizing electron energies. Figure 5 also shows the relative yield of Cl_2^{2+} via dissociative double ionization [Eq. (15)] which is a significant contribution to the total ion yield. Consistent with the relative partial ionization cross section data discussed in the preceding paragraph, the threshold for Cl_2^{2+} formation by double ionization lies between 40 and 45 eV.

Figure 6 shows the relative cross section for forming Cl^+ via dissociative double ionization [Eq. (16)]. We see that the formation of Cl^+ by this pathway peaks at ~ 100 eV and has a threshold at 35 ± 2 eV. Figure 6 also shows the relative yield of Cl_2^{2+} via dissociative triple ionization [Eq. (17)]. Of course, this cross section is equal to the cross section for the formation of Cl^+ by triple ionization as the dissociative triple ionization process must form Cl^+ if it forms Cl_2^{2+} . The threshold for formation of Cl_2^{2+} by dissociative triple ioniza-

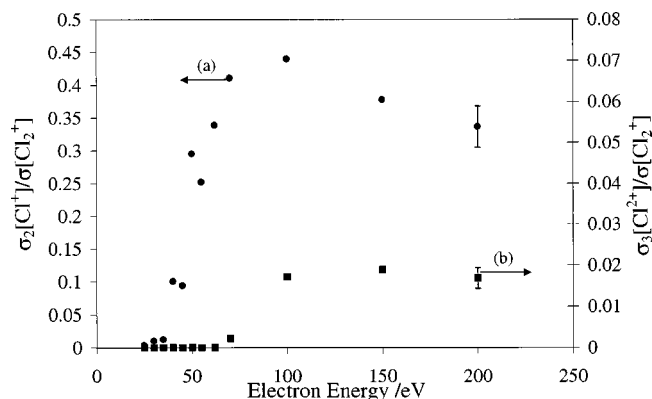


FIG. 6. Cross sections for forming (a) Cl^+ via dissociative double ionization and (b) Cl_2^{2+} via dissociative triple ionization following electron-impact ionization of Cl_2 . These cross sections are expressed relative to the cross section for forming Cl_2^+ . Representative error bars are shown in the figure.

tion, which is clearly above 62 eV is estimated to be 65.3 ± 2 eV.

No Cl_2^{2+} signals were observed in the mass spectrum, despite such ions being detected before and the mixed isotopomer $^{35}\text{Cl}^{37}\text{Cl}_2^{2+}$ having a m/z value which is not common to any other ion in the spectrum.³⁰ However, the weak Cl_2^{2+} signals are undoubtedly buried under the intense Cl^+ signals in the TOF mass spectrum (Fig. 2). These Cl^+ signals are also broad, as a significant number of these fragments have a significant translational energy, making any Cl_2^{2+} signals hard to observe.

At an ionizing electron energy of 200 eV weak signals due to Cl_2^{3+} are clearly visible (Fig. 2) in the singles spectrum. The signals have the correct isotopic distribution and occur at precisely the expected time of flight in all spectra recorded at 200 eV. The Cl_2^{3+} ion has been observed following strong field laser ionization, but never reported as a product of simple electron-impact ionization.⁵⁶ The yield of Cl_2^{3+} at 200 eV gives a $\sigma_r[\text{Cl}_2^{3+}/\text{Cl}_2^+]$ value of 4×10^{-4} . Thus, the relative yield of long-lived triply-charged ions to dissociative triple ionization is 1:50. In the laser studies, which investigated ionization of the halogens, the ratio of stable I_2^{3+} formation with respect to dissociative I_2^{3+} formation was at best 1:450 and the authors indicate the corresponding ratio for Cl_2^{3+} was even more strongly in favor of dissociative triple ionization.⁵⁶ Hence, our results show that long-lived triply-charged ion formation by electron-impact ionization of chlorine is more probable than by strong field laser ionization.

Very weak signals corresponding to the ion pair $\text{Cl}^{2+} + \text{Cl}^{2+}$, formed by quadruple ionization of Cl_2 , were just visible in the pairs spectrum at 200 eV electron energy. Given the low intensity of these signals (98 pairs from the total of 22018) the neglect of quadruple ionization at the electron energies employed in this study is justified.

B. Kinetic energy release measurements

The kinetic energy release for the dissociative ionization processes forming $\text{Cl}^+ + \text{Cl}^+$ and $\text{Cl}^+ + \text{Cl}_2^{2+}$ were determined at several electron energies. This analysis was performed, as described above, by selecting the pairs making up the reac-

TABLE I. Kinetic energy release (KER) values, with their associated uncertainty δ_{KER} and Gaussian widths w , required to model the experimental coincidence signals. See the text for details.

Electron energy/eV	$\text{Cl}^+ + \text{Cl}^+$			$\text{Cl}^+ + \text{Cl}_2^{2+}$		
	KER/eV	$\delta_{\text{KER}}/\text{eV}$	w/eV	KER/eV	$\delta_{\text{KER}}/\text{eV}$	w/eV
35	4.4	± 0.2	2.8	^a		
50	6.0	± 0.3	3.0	^a		
70	6.1	± 0.3	3.0	^a		
100	6.1	± 0.3	3.0	10.0	± 0.6	2.7
200	6.2	± 0.3	3.2	10.0 and 16.0	$\pm 0.6, \pm 1.0$	3.0

^aInsufficient signal to allow a statistically significant estimate of the KER.

tion of interest and forming from those pairs a time-of-flight difference spectrum ($t_2 - t_1$). This spectrum is then compared with a spectrum produced by a Monte-Carlo algorithm. The Monte-Carlo algorithm includes all the experimental parameters and allows the kinetic energy release to be varied until there is satisfactory agreement with the experimental data.^{46,49,50} A representative selection of the energy releases determined are shown in Table I. At all the electron energies employed in this study the KER for the $\text{Cl}^+ + \text{Cl}^+$ channel could be well modeled by a single-valued energy release, whereas at the higher electron energies two distinct KERs were required to satisfactorily model the $\text{Cl}^+ + \text{Cl}_2^{2+}$ channel. Note that, as discussed below, the fact that the $\text{Cl}^+ + \text{Cl}^+$ channel can be well modeled by a single Gaussian energy release does not mean that only one dissociative state is contributing to the coincidence signal.

IV. DISCUSSION

A. Ionization yields

1. Cl^+ formation

The formation of Cl^+ from Cl_2 has a threshold^{19,20} which is below the lowest electron energy employed in the current work and is thus not visible in Fig. 4. At electron energies from 50 to 150 eV the relative partial ionization cross section shows (Fig. 4) that there are almost as many Cl^+ ions formed as Cl_2^+ ions. However, the yield for Cl^+ from double ionization (Fig. 6) clearly shows that above 50 eV a considerable fraction of these Cl^+ ions are from multiple ionization and, hence, may be detected with low efficiency using a quadrupole or conventional magnetic sector mass spectrometer. Figure 5(a) shows that the yield of Cl^+ from single ionization reaches a maximum at around 40 eV, but even in this energy regime the yield of Cl^+ from single ionization is only a factor of 2–3 times the yield from double ionization. Thus, this data confirms that experiments must be sure to gather energetic ions efficiently to make accurate assessments of partial ionization cross sections as such ions can be a major component of the ion yield. Similar conclusions have been drawn from recent studies of the ionization of CF_4 where at 200 eV multiple ionization accounts for 40% of the ion yield.^{11–13}

Figure 6(a) shows the threshold for the formation of Cl^+ by dissociative double ionization lies at 35 ± 2 eV, in agreement with an earlier precursor state determination (33.2

± 0.2 eV) via kinetic energy release measurements, which in principle are capable of significantly greater precision than our threshold determination.³²

2. Cl_2^{2+} formation

The partial ionization cross section for formation of Cl^{2+} (Fig. 4) shows that these ions contribute a few percent of the ion yield at energies above 50 eV. Our estimate of the threshold for Cl^{2+} formation (~ 42 eV) lies well below the onset of dissociative triple ionization (~ 65 eV, Fig. 6) and we feel our data conclusively show that Cl_2^{2+} decays by neutral loss to form $\text{Cl}^{2+} + \text{Cl}$ as well as via charge separation to form $\text{Cl}^+ + \text{Cl}^+$. The data show that the neutral loss channel makes up about 5% of the dicationic dissociations detected. The observed threshold for Cl^{2+} formation via double ionization is at a higher energy than any states of Cl_2^{2+} which have been investigated theoretically so it is not possible to speculate on the identity of the state of Cl_2^{2+} which dissociates to form Cl^{2+} . The asymptote for the formation of Cl^{2+} and Cl in their ground states is 38.1 eV^{57,58} and, reassuringly, our estimate of the fragmentation threshold is certainly above this thermodynamic limit.

The yield of Cl^{2+} from dissociative triple ionization is obviously equal to the yield of Cl^+ by the same route ($\sigma_3[\text{Cl}^+]/\sigma[\text{Cl}_2^+] = \sigma_3[\text{Cl}^{2+}]/\sigma[\text{Cl}_2^+]$) and Fig. 6 shows that dissociative triple ionization contributes a few percent, a minor but significant fraction, to the ion yield above 100 eV. The threshold at 65.3 eV for the formation of Cl^+ via triple ionization (Fig. 6) provides the first estimate of the triple ionization potential of Cl_2 . In principle this estimate will be an upper limit as long-lived states of Cl_2^{3+} may lie below the onset of dissociative triple ionization. However, calculations^{56,59} show that the metastable state of Cl_2^{3+} has only a shallow minimum and, hence, the onset of dissociative triple ionization should lie at worst only about 0.4 eV above the triple ionization potential, well within our error limits.

B. Kinetic energy release measurements

As described above, by adding the KER for a given charge-separating dissociation to the energy of the relevant dissociation asymptote, we determine an estimate of the energy of the multiply charged ion state(s) which are undergoing the dissociative process.

1. $\text{Cl}_2^{2+} \rightarrow \text{Cl}^+ + \text{Cl}^+$

The first 3 electronic states of Cl_2^{2+} , arising from the $\sigma_g^2 \pi_u^4 \pi_g^2$ configuration, support long-lived vibrational levels. The population of these states has been observed directly in photoionization experiments and the appearance energy of the $\nu=0$ level of the $X^3\Sigma_g^-$ ground state has been determined to be 31.13 eV.³⁴ The population of higher lying states of Cl_2^{2+} has been detected via double-charge transfer experiments and compared with theoretical calculations of the energies of the dication states.³³ Experiments performed in the 1960's gave a value of 32.6 eV for the appearance energy of long-lived Cl_2^{2+} ions.³⁰ This appearance potential was assigned by Fournier *et al.*³³ to the formation of the $1^1\Sigma_u^-$

electronic state arising from the $\sigma_g^2 \pi_u^3 \pi_g^3$ configuration, which they calculated to possess a shallow minima. If this assignment is correct then it appears that, perhaps surprisingly, electron-impact ionization does not favor the population any of the Cl_2^{2+} states arising from the $\sigma_g^2 \pi_u^4 \pi_g^2$ configuration. More recent theoretical work by McConkey *et al.*³⁴ has shown that the calculations of Fournier *et al.*,³³ as the authors indeed noted, produced absolute energies of the dicationic states which were about 0.5 eV too low. This recent theoretical and experimental work³⁴ shows that the $\sigma_g^2 \pi_u^4 \pi_g^2 b^1\Sigma_g^+$ state lies at 32.1 eV and the $1^1\Sigma_u^-$ state at 33.0 eV, both within the error bar of the Cl_2^{2+} appearance potential.³⁰ Hence, either state could be the source of long-lived Cl_2^{2+} ions. Measurements on the dissociation of long-lived Cl_2^{2+} ions in a dual sector mass spectrometer³² determined a KER of 4.79 eV which, assuming that this dissociation forms ground state products, results from a dication state lying at 33.2 eV above the ground state of Cl_2 .⁵⁷ Again, these dissociations could be from the $1^1\Sigma_u^-$ electronic state, or a high-lying vibrational level of the $b^1\Sigma_g^+$ state. The latter state has a calculated well depth⁵⁹ of 0.78 eV, placing the top of the barrier to its dissociation at 32.9 eV, within the error bar of the KER determination. It certainly seems likely, since both experiments employ electron-impact ionization, that the energetics derived from the appearance potential for long-lived dications and the KER from the dissociation of long-lived dications relate to the same electronic state but definitive assignment to the $b^1\Sigma_g^+$ or the $1^1\Sigma_u^-$ is not possible.

At high electron energies (Table I), our $\text{Cl}^+ + \text{Cl}^+$ data are well modeled by a KER of 6 eV, but at 35 eV ionizing energy the best fit is for a release of 4.4 ± 0.2 eV. Undoubtedly at the higher electron energies several dissociative states are contributing to the $\text{Cl}^+ + \text{Cl}^+$ coincidence signals, but these separate contributions cannot be resolved in the spectrum. However, at 35 eV we can only populate low-lying states of Cl_2^{2+} and the KER at this ionizing energy corresponds to a Cl_2^{2+} state lying at 32.8 eV, in good agreement with our threshold (35 ± 2 eV) for the formation of Cl^+ by dissociative double ionization (Fig. 6) and close to the calculated energy for the top of the $b^1\Sigma_g^+$ well or the $1^1\Sigma_u^-$ electronic state. Hence, our work does not further clarify the assignment of these signals. Despite the well depth of the $b^1\Sigma_g^+$ state being sufficient to support several vibrational levels, no evidence for discrete vibrational levels was observed in the TPEsCO signals attributed to this state. Hence, it certainly is a possible source for the fragmentations which are observed. Higher resolution (Doppler-free) KER measurements are required to try and resolve which state is populated. If electron impact ionization does not populate any levels arising from the $\sigma_g^2 \pi_u^4 \pi_g^2$ configuration such selectivity also requires an explanation.

2. $\text{Cl}_2^{3+} \rightarrow \text{Cl}^{2+} + \text{Cl}^+$

This dissociation reaction has not been studied before. As shown in Table I, there is only a sufficient coincidence signal in the pairs spectra at 100 eV and 200 eV to allow a statistically significant estimate of the KER to be made. At an electron energy of 100 eV, 35 eV above the triple ioniza-

tion energy, a KER of 10 ± 0.6 eV is apparent. While at 200 eV two energy releases are clearly visible: 10 ± 0.6 eV and 16 ± 1.0 eV. The thermodynamic asymptote for the products of this dissociation reaction ($\text{Cl}_2^{2+} + \text{Cl}^+$) lies 52.3 eV above the ground state of Cl_2 .^{57,58} Hence, our KER values correspond to trication state energies of 62.3 and 68.3 eV, if ground state products are formed. However, since the KER of 16 eV is not apparent in the spectrum at 100 eV ionizing energy, it is certainly possible that this release corresponds to the formation of products in electronically excited states and, hence, the precursor state energy of 68.3 eV must be viewed with some caution. In contrast, it is satisfying to note that the precursor energy derived from the 10 eV release (62.3 ± 0.6 eV) is in good agreement with the threshold (63.5 ± 2 eV, Fig. 6) derived from $\sigma_3[\text{Cl}_2^{2+}]/\sigma[\text{Cl}_2^+]$, which indicates that the $\text{Cl}_2^{2+} + \text{Cl}^+$ products are most probably formed in their ground electronic states. The trication state responsible for the formation of $\text{Cl}_2^{2+} + \text{Cl}^+$ at these ionizing energies, close to the triple threshold, may well be the ground ($^2\Pi_g$) state of the dication.^{56,59} This electronic state is almost certainly the source of the long-lived triply-charged ions observed in our experiments and via strong-field laser ionization. However, although there are undoubtedly some metastable vibrational levels supported in the $^2\Pi_g$ electronic state,⁵⁹ it is certainly possible that the dissociative processes may arise either by populating high-lying $^2\Pi_g$ vibrational states or by predissociation of $^2\Pi_g$ vibrational states via a curve crossing with a repulsive excited state⁵⁹ of Cl_2^{3+} or by population of a portion of the potential energy curve lying above the barrier to charge separation.⁶⁰ The tunneling lifetime of the highest vibrational level of the $^2\Pi_g$ state has been calculated to be 160 ns.⁵⁶ However, more recent calculations with a larger basis set indicate that the potential energy curve used for these lifetime calculations is not optimal.⁵⁹ Our signals must arise predominantly from ions dissociating on timescales shorter than 10 ns, otherwise characteristic tails on the coincidence peaks would be seen in the pairs spectrum. However, it is well known that the lifetimes of metastable states of multiply-charged ions are often shorter than the “tunneling lifetime,” due to predissociative curve crossings. Such crossings may well reduce the lifetime of high vibrational states of the $^2\Pi_g$ state of Cl_2^{2+} making such levels the source of the rapid dissociations to $\text{Cl}_2^{2+} + \text{Cl}^+$ we observe.

V. CONCLUSIONS

Two-dimensional time-of-flight mass spectra have been recorded to determine the relative partial ionization cross-sections for the formation of Cl_2^+ , Cl^+ and Cl_2^{2+} from molecular chlorine as a function of the ionizing electron energy. These measurements could be placed on an absolute scale by comparison with the total ionization cross section.⁶

The partial ionization cross sections show that at electron energies above the double ionization threshold, when high energy fragment ions are collected efficiently, the yield of fragment ions (Cl^+ , Cl_2^{2+}) can be comparable with the ion yield of Cl_2^+ from nondissociative ionization. These data can also be analyzed, together with a determination of the ion detection efficiency, to give contribution of single, double

and triple ionization to the yield of each of the ions detected. This analysis shows that, at electron energies above 50 eV, the yield of fragment ions from multiple ionization is comparable with the yield of fragment ions from single ionization. Indeed, dissociative multiple ionization contributes 14% of the ion yield at 50 eV electron energy and 26% at 100 eV; a contribution to the ion yield which means that the energetic ions from dissociative multiple ionization cannot be neglected when determining partial ionization cross sections above the double ionization potential.

The decay of Cl_2^{2+} via heterolytic cleavage to form Cl^{2+} is a fate of approximately 5% of the dissociative double ionization events and has a threshold at 41.8 ± 1.5 eV. Such heterolytic cleavage is not normally considered in theoretical investigations of small multiply-charged ions and a computational search for the states responsible for this dissociation would be valuable. Electron-impact induced triple ionization for long-lived Cl_2^{3+} ions has been detected for the first time. This nondissociative triple ionization process makes up approximately 2% of the triple ionization events, and triple ionization in total is responsible for approximately 2% of the ion yield above 100 eV. The threshold for dissociative triple ionization is determined, by measurements of the variation of the ion pair yield and a determination of the kinetic energy release in the charge-separating fragmentation of Cl_2^{3+} , to be 65.3 ± 1.5 eV. This provides the first experimental estimate of the triple ionization energy of molecular chlorine.

ACKNOWLEDGMENTS

The authors gratefully acknowledge the financial support of the University of London for these experiments, University College London for their support of the visit of P.C. and the award of an EPSRC studentship for C.S.S.O.

- ¹ *Plasma Etching*, edited by D. M. Manos and D. L. Flamm (Academic, Boston, 1989).
- ² G. L. Rogoff, J. M. Kramer, and R. B. Piejak, *IEEE Trans. Plasma Sci.* **14**, 103 (1986).
- ³ E. S. Aydil and D. J. Economou, *J. Electrochem. Soc.* **139**, 1396 (1992).
- ⁴ P. L. G. Ventzek, M. Grapperhaus, and M. J. Kushner, *J. Vac. Sci. Technol. B* **12**, 3118 (1994).
- ⁵ M. J. Kushner, *J. Appl. Phys.* **82**, 5312 (1997).
- ⁶ L. G. Christophorou and J. K. Olthoff, *J. Phys. Chem. Ref. Data* **28**, 131 (1999).
- ⁷ T. D. Mark, in *Electron Impact Ionization*, edited by T. D. Mark and G. H. Dunn (Springer-Verlag, New York, 1985), p. 137.
- ⁸ D. Margreiter, G. Walder, H. Deutsch, H. U. Poll, C. Winkler, K. Stephan, and T. D. Mark, *Int. J. Mass Spectrom. Ion Processes* **100**, 143 (1990).
- ⁹ M. V. V. S. Rao and S. K. Srivastava, *J. Phys. B* **25**, 2175 (1992).
- ¹⁰ H. U. Poll, C. Winkler, D. Margreiter, V. Grill, and T. D. Mark, *Int. J. Mass Spectrom. Ion Processes* **112**, 1 (1992).
- ¹¹ C. Ma, M. R. Bruce, and R. A. Bonham, *Phys. Rev. A* **44**, 2921 (1991).
- ¹² M. R. Bruce and R.-A. Bonham, *Int. J. Mass Spectrom. Ion Processes* **123**, 97 (1993).
- ¹³ M. R. Bruce, L. Mi, C. R. Sporleder, and R. A. Bonham, *J. Phys. B* **27**, 5773 (1994).
- ¹⁴ B. P. Tsai and J. H. D. Eland, *Int. J. Mass Spectrom. Ion Processes* **36**, 143 (1980).
- ¹⁵ P. Lablanquie, I. Nenner, P. Millie, P. Morin, J. H. D. Eland, M. J. Hubin-Franskin, and J. Delwiche, *J. Chem. Phys.* **82**, 2951 (1985).
- ¹⁶ J. H. D. Eland, F. S. Wort, and R. N. Royds, *J. Electron Spectrosc. Relat. Phenom.* **41**, 297 (1986).
- ¹⁷ P. A. Hatherly, M. Stankiewicz, L. J. Frasinski, K. Codling, and M. A. Macdonald, *Chem. Phys. Lett.* **159**, 355 (1989).

- ¹⁸M. R. Bruce and R. A. Bonham, *Z. Phys. D: At., Mol. Clusters* **24**, 149 (1992).
- ¹⁹D. C. Frost and C. A. McDowell, *Can. J. Phys.* **38**, 407 (1960).
- ²⁰R. Thorburn, *Proc. Phys. Soc. London* **123**, 122 (1959).
- ²¹D. Mathur, *Phys. Rep.* **225**, 193 (1993).
- ²²S. D. Price, *J. Chem. Soc., Faraday Trans.* **93**, 2451 (1997).
- ²³D. Schroder and H. Schwarz, *J. Phys. Chem. A* **103**, 7385 (1999).
- ²⁴C. P. Safvan, M. Krishnamurthy, and D. Mathur, *J. Phys. B* **26**, L837 (1993).
- ²⁵T. Weiske, W. Koch, and H. Schwarz, *J. Am. Chem. Soc.* **115**, 6312 (1993).
- ²⁶K. A. Newson and S. D. Price, *Chem. Phys. Lett.* **294**, 223 (1998).
- ²⁷J. Zabka, M. Farnik, Z. Dolejssek, and Z. Herman, *Int. J. Mass Spectrom. Ion. Processes* **187**, 195 (1999).
- ²⁸A. Ehbrecht, N. Mustafa, C. Ottinger, and Z. Herman, *J. Chem. Phys.* **105**, 9833 (1996).
- ²⁹E. Y. Kamber, K. Akgungor, C. P. Safvan, and D. Mathur, *Chem. Phys. Lett.* **258**, 336 (1996).
- ³⁰J. T. Herron and V. H. Dibeler, *J. Chem. Phys.* **32**, 1884 (1960).
- ³¹A. C. Hurley and V. W. Maslen, *J. Chem. Phys.* **34**, 1919 (1961).
- ³²J. H. Beynon, R. M. Caprioli, and J. W. Richardson, *J. Am. Chem. Soc.* **93**, 1852 (1971).
- ³³P. G. Fournier, J. Fournier, F. Salama, D. Stark, S. D. Peyerimhoff, and J. H. D. Eland, *Phys. Rev. A* **34**, 1657 (1986).
- ³⁴A. G. Mcconkey, G. Dawber, L. Avaldi, M. A. Macdonald, G. C. King, and R. I. Hall, *J. Phys. B* **27**, 271 (1994).
- ³⁵W. C. Wiley and I. H. McLaren, *Rev. Sci. Instrum.* **26**, 1150 (1955).
- ³⁶J. H. D. Eland, *Mol. Phys.* **61**, 725 (1987).
- ³⁷S. Hsieh and J. H. D. Eland, *J. Phys. B* **30**, 4515 (1997).
- ³⁸S. Hsieh and J. H. D. Eland, *Int. J. Mass Spectrom.* **167**, 415 (1997).
- ³⁹V. R. Bhardwaj, K. Vijayalakshmi, and D. Mathur, *J. Phys. B* **32**, 1087 (1999).
- ⁴⁰M. Foltin, G. J. Stueber, and E. R. Bernstein, *J. Chem. Phys.* **109**, 4342 (1998).
- ⁴¹D. A. Card, D. E. Folmer, S. Sato, S. A. Buzza, and A. W. Castleman, *J. Phys. Chem. A* **101**, 3417 (1997).
- ⁴²L. J. Frasinski, A. J. Giles, P. A. Hatherly, J. H. Posthumus, M. R. Thompson, and K. Codling, *J. Electron Spectrosc. Relat. Phenom.* **79**, 367 (1996).
- ⁴³P. Jukes, A. Buxey, A. B. Jones, and A. J. Stace, *J. Chem. Phys.* **109**, 5803 (1998).
- ⁴⁴D. A. Hagan and J. H. D. Eland, *Org. Mass Spectrom.* **27**, 855 (1992).
- ⁴⁵L. J. Frasinski, M. Stankiewicz, P. A. Hatherly, and K. Codling, *Meas. Sci. Technol.* **3**, 1188 (1992).
- ⁴⁶C. S. O'Connor and S. D. Price, *Int. J. Mass Spectrom. Ion Processes* **184**, 11 (1999).
- ⁴⁷D. S. Belic and M. V. Kurepa, *J. Phys. B* **11**, 3719 (1978).
- ⁴⁸M. R. Bruce, C. Ma, and R. A. Bonham, *Chem. Phys. Lett.* **190**, 285 (1992).
- ⁴⁹C. S. S. O'Connor, N. Tafadar, and S. D. Price, *J. Chem. Soc., Faraday Trans.* **94**, 1797 (1998).
- ⁵⁰C. S. S. O'Connor and S. D. Price, *Int. J. Mass Spectrom. Ion Processes* **113**, 119 (1998).
- ⁵¹S. Hsieh and J. H. D. Eland, *J. Chem. Phys.* **103**, 1006 (1995).
- ⁵²M. Lundqvist, D. Edvardsson, P. Baltzer, and B. Wannberg, *J. Phys. B* **29**, 1489 (1996).
- ⁵³S. Hsieh and J. H. D. Eland, *J. Phys. B* **29**, 5795 (1996).
- ⁵⁴R. I. Hall, L. Avaldi, G. Dawber, A. G. Mcconkey, M. A. Macdonald, and G. C. King, *Chem. Phys.* **187**, 125 (1994).
- ⁵⁵J. A. R. Samson and G. C. Angel, *J. Chem. Phys.* **86**, 1814 (1987).
- ⁵⁶H. Sakai, H. Stapelfeldt, E. Constant, M. Y. Ivanov, D. R. Matusek, J. S. Wright, and P. B. Corkum, *Phys. Rev. Lett.* **81**, 2217 (1998).
- ⁵⁷S. G. Lias, R. D. Levin, and S. A. Kafafi, in *NIST Chemistry WebBook*, NIST Standard Reference Database Number 69 (<http://webbook.nist.gov>), edited by W. G. Mallard and P. J. Linstrom (National Institute of Standards and Technology, Gaithersburg, MD, 1998).
- ⁵⁸*NIST Atomic Spectra Database 2.0* (<http://physics.nist.gov/>), Atomic Energy Levels Data Center, NIST.
- ⁵⁹J. S. Wright, G. A. Dilabio, D. R. Matusek, P. B. Corkum, M. Y. Ivanov, C. Ellert, R. J. Buenker, A. B. Alekseyev, and G. Hirsch, *Phys. Rev. A* **59**, 4512 (1999).
- ⁶⁰P. Champkin, N. Kaltsoyannis, and S. D. Price, *J. Electron Spectrosc. Relat. Phenom.* **105**, 21 (1999).